Quantitative Characterization of Membrane Binding of Peripheral Proteins by Spin-Label EPR Spectroscopy

Suren A. Tatulian*

Biomolecular Science Center, University of Central Florida, 12722 Research Parkway, Orlando, Florida 32826

Received: May 1, 2002; In Final Form: June 19, 2002

Key enzymes involved in transmembrane signaling and lipid metabolism (e.g., protein kinase C and phospholipases A_2, C, and D) are activated by binding to cellular membranes. Elucidation of the molecular mechanisms of these peripheral membrane proteins requires detailed characterization of their interactions with membrane lipids. Previously, EPR studies on protein−membrane interactions have been analyzed using a formalism for integral membrane proteins, permitting determination of the lipid-to-protein stoichiometry (N) and the relative affinity of the labeled versus unlabeled lipids for the protein (K_r). Here, a formalism is developed that permits a comprehensive description of the membrane binding of peripheral proteins. The interaction of an interfacially activated enzyme, secretory phospholipase A_2 (PLA_2), with membranes containing spin-labeled lipids is studied by EPR spectroscopy. Under noncatalytic conditions, binding of PLA_2 to fluid membranes (order parameter $S_{zz} \approx 0.24$) causes the formation of a second, immobilized lipid component with $S_{zz} \approx 0.80$. Under catalytic conditions, a third, more mobile component is observed that is evidently generated by the lipid hydrolysis product, lysophospholipid. In addition to N and K_r, the new theory allows the determination of the following parameters: the fraction of protein-accessible lipids (f), the membrane-binding constant of PLA_2 (K), the fraction of the labeled lipids associated with a membrane-bound protein (n_r), and the microscopic Gibbs free energies of protein binding of labeled (ΔG_{lab}) and unlabeled lipids (ΔG_{unlab}). The experimental and theoretical approaches described in this work expand the limits of characterization of protein−lipid interactions by EPR spectroscopy.

Introduction

Peripheral membrane proteins such as protein kinase C and phospholipases A_2, C, and D act as key players in various membrane-mediated cell functions including but not limited to transmembrane signaling, lipid metabolism, membrane trafficking, and phagocytosis.[1−6] Membrane binding results in a substantial increase in the activity of these enzymes and hence regulates their function. There is increasing evidence that interfacial activation is very sensitive to the mode of enzyme−membrane interactions, such as the strength of binding, lipid-to-protein stoichiometry, and lipid specificity (see above references). Obviously, the molecular mechanisms of these and other peripheral membrane proteins can be understood only on the basis of detailed quantitative characterization of their interactions with membrane lipids.

Spin-label electron paramagnetic resonance (EPR) spectroscopy has been used to analyze interactions with membrane lipids of both integral[7−11] and peripheral proteins and peptides.[12−16] The general experimental design is to use a small fraction of a spin-labeled lipid in the membrane and measure protein-induced changes in the EPR spectra due to binding to the protein and immobilization of the lipid. A theoretical formalism was developed by Brotherus et al.[17] to characterize the interaction of integral proteins with membranes by an analysis of the EPR spectra. This approach takes advantage of the fact that all of the integral protein in the system is incorporated into the membrane, and therefore the actual molar ratio of the lipid to the membrane-bound protein is the same as the input lipid-to-protein ratio. Consequently, the ratio of the free to protein-bound lipids is a linear function of the lipid-to-protein ratio. Then, the slope and x or y intercepts of this linear dependence are used to determine two parameters, the lipid-to-protein binding stoichiometry (N) and the relative affinity of the labeled versus unlabeled lipids for the protein (K_r). The situation with water-soluble proteins is more complex because typically a large fraction of the total protein is free in the buffer and the concentration of the membrane-bound protein is a nonlinear function of the total protein concentration. Although it was recognized more than 20 years ago that the above theory cannot be applied to the interactions of water-soluble proteins with membranes,[17] so far no theoretical model has been developed to characterize quantitatively the membrane binding of peripheral proteins using spin-labeled EPR data.

Here, the interaction of an interfacially activated enzyme, secretory phospholipase A_2 (PLA_2), with membranes containing spin-labeled lipids is studied by EPR spectroscopy. Under noncatalytic conditions, the binding of PLA_2 to fluid membranes (order parameter $S_{zz} \approx 0.24$) causes the formation of a second, immobilized lipid component with $S_{zz} \approx 0.80$. Under catalytic conditions, a third, more mobile component is observed, which is evidently generated by the lipid hydrolysis product, lysophospholipid. A formalism is developed that allows a detailed description of membrane binding of *peripheral* proteins. In addition to N and K_r, the new theory permits the determination of the following parameters: the fraction of protein-accessible lipids (f), the binding constant of PLA_2 for the membrane containing both labeled and unlabeled lipids (K) and for membranes of pure unlabeled lipids (K_{POPC}), the fraction of the

* E-mail: statulia@mail.ucf.edu. Tel.: (407) 207-4996 or (407) 207-4976. Fax: (407) 384-2816.

10.1021/jp026052n CCC: $22.00
Published on Web 07/31/2002

labeled lipids associated with a membrane-bound protein (n_r), and the microscopic Gibbs free energies of the protein binding of labeled (ΔG_{lab}) and unlabeled lipids (ΔG_{unlab}). The results of this work provide new theoretical tools to characterize quantatively interactions with membranes of peripheral proteins on the basis of spin-labeled EPR data.

Theory

Protein−lipid interactions can be visualized by spin-label EPR spectroscopy, provided binding of the protein to the membrane results in the appearance of a new component in the EPR spectra, which is generated by the fraction of the lipids that interact with the protein. The purpose of this section is to derive analytic expressions that will be used to characterize the binding of peripheral proteins to membranes on the basis of the dependence of the fraction of immobilized lipids on protein concentration.

Let us first consider a system where all the protein is bound to membranes, which is the case for integral proteins. At a given lipid-to-protein molar ratio, the numbers of protein-bound and free lipids per protein are respectively N and $n_b - N$, where n_b is the total number of lipids per membrane-bound protein and N is the number of lipids that interact with a membrane-bound protein. The molar ratio of free and protein-bound lipids is

$$\frac{L_f}{L_b} = \frac{n_b - N}{N} \tag{1}$$

where L_f and L_b are the fractions of free and protein-bound lipids, respectively, per membrane-bound protein. In a typical experiment, the membrane is composed of a host lipid and a small fraction of spin-labeled lipids. If the labeled and unlabeled lipids have different affinities for the protein, the ratio of free to bound labeled lipids will simply be

$$\frac{L_f^*}{L_b^*} = \frac{1}{K_r}\left(\frac{n_b}{N} - 1\right) \tag{2}$$

where K_r is defined as

$$K_r = \frac{L_b^* L_f}{L_f^* L_b} \tag{3}$$

In eqs 2 and 3, the asterisk indicates the labeled lipid. Equation 2 has been derived previously and used to describe the interaction of integral proteins with membrane lipids.[17] For integral proteins, n_b is directly determined by the experiment as the input lipid-to-protein molar ratio, $n_b = x \equiv L_t/P_t$, where L_t and P_t are the total lipid and protein concentrations, respectively. The ratio L_f^*/L_b^* is determined from the line shape of the EPR spectra (see below). Then, from the linear dependence of L_f^*/L_b^* versus n_b (eq 2), the parameters K_r and N are determined.

Because integral proteins are not water soluble, all the protein is in the membrane, and because they span the membrane, each lipid molecule in the membrane is able to interact with the protein. The main differences between integral and peripheral proteins are that (i) in the latter case, only a fraction $f < 1$ of the lipids in the external leaflet of vesicle membranes is accessible to the externally added protein and (ii) only a fraction of the protein is membrane-bound. The task is to obtain an equation for the dependence of the proportions of *total* free and protein-bound lipids on the *total* lipid-to-protein molar ratio (i.e., an analogue of eq 2 for peripheral proteins). For peripheral proteins, there are three populations of the lipids: (i) the fraction of lipids ($1 - f$) that is not accessible to the protein (such as the lipids in the internal leaflet), (ii) the fraction (L_f) that is protein-accessible but does not interact with the protein at a given protein concentration because protein binding is not yet saturated, and (iii) the fraction of the lipids that are protein-accessible and are bound to the protein (L_b). By definition, $L_f + L_b = f$. For a multicomponent membrane, this relationship is true for any lipid species, implying that $L_f^* + L_b^* = f$. It should be understood that L_f^* and L_b^* are the fractions of protein-accessible free and bound labeled lipids. In eq 2, this is not specified because eq 2 applies to integral proteins when all lipids are protein-accessible. This, in combination with eq 2, gives $L_b^* = f/[1 + (n_b/N - 1)/K_r]$. As noted above, in addition to the protein-accessible free lipid (L_f^* in eq 2), a protein-inaccessible fraction ($1 - f$) of the total lipids is always free (i.e., the fraction of the total free lipids is $1 - f + L_f^*$). (Here we consider only the labeled lipids because only the labeled lipids contribute to the EPR spectra). These considerations lead directly to the following expression for the molar ratio of the overall free and protein-bound lipids:

$$y \equiv \frac{L_{f,total}^*}{L_b^*} = \frac{1 + \frac{1}{K_r}\left(\frac{n_b}{N} - 1\right)}{f} - 1 \tag{4}$$

It has been shown previously that membrane binding of peripheral proteins, including secretory PLA_2, can be described by the Langmuir adsorption isotherm,[18] which can be presented in the form

$$\frac{P_b}{L_{acc}} = \frac{\frac{1}{N}KP_f}{1 + KP_f} \tag{5}$$

where L_{acc} is the concentration of the lipids that are accessible for protein binding, P_b and P_f are the concentrations of membrane-bound and free protein, respectively, and K is the binding affinity of the protein for the membrane. Taking into account that $L_{acc} = fL_t$, $n_b \equiv L_{acc}/P_b$, and $P_f = P_t - P_b$ and replacing P_b by fL_t/n_b, eq 5 can be presented as a quadratic equation with respect to n_b

$$n_b^2 - an_b + fNx = 0 \tag{6}$$

and solved as

$$n_b = \frac{a}{2} \pm \sqrt{\frac{a^2}{4} - fNx} \tag{7}$$

where

$$a \equiv fx + \frac{Nx}{KL_t} + N$$

It should be noted that only the plus sign in front of the square root in eq 7 should be used because the negative sign yields physically meaningless (negative) values for L_f^*/L_b^*. Thus, by insertion of n_b from eq 7 into eq 4, we obtain an equation for the dependence of the mole ratio of the total free to protein-bound lipids (parameter y) on the overall lipid-to-protein ratio (parameter x):

$$y = \frac{1}{fK_r}\left(\frac{a}{2N} + \frac{1}{N}\sqrt{\frac{a^2}{4} - fNx} + K_r - 1\right) - 1 \qquad (8)$$

As shown below, analysis of this relationship can yield four parameters that characterize the interaction of a peripheral protein with the membrane: f, K_r, K, and N. Furthermore, having determined these parameters, the fraction of the labeled lipids associated with a membrane-bound protein (n_r), the binding constant of the protein for membranes of pure unlabeled lipids (K_{POPC}), and the microscopic Gibbs free energies of protein binding of labeled (ΔG_{lab}) and unlabeled lipids (ΔG_{unlab}) will be evaluated.

A simulated $y(x)$ dependence is presented in Figure 1 for illustration of the peculiarities of this relationship. It follows from eq 8 that at high protein concentration ($x \rightarrow 0$), $y = 1/f - 1$. This implies that the fraction of protein-accessible lipids can be found from the intersection of the $y(x)$ dependence with the y axis as

$$f = \frac{1}{1 + y_{0,1}} \qquad (9)$$

where $y_{0,1}$ can be determined experimentally by extrapolating the $y(x)$ dependence to $x = 0$, as shown in Figure 1.

At low protein concentrations (i.e., for large x), when $KP_f \ll 1$, eq 5 reduces to $n_b = N/KP_f$. After the following substitutions—$P_f = P_t - P_b$, $P_t = L_t/x$, and $P_b = fL_t/n_b$—we arrive at $n_b = x(N/KL_t + f)$, which is inserted into eq 4 to yield

$$y = \frac{x}{K_r}\left(\frac{1}{KL_t f} + \frac{1}{N}\right) - \frac{1}{K_r f} + \frac{1}{f} - 1 \qquad (10)$$

Equation 10 demonstrates that at low protein concentrations y is a linear function of x, with an intercept of $y_{0,2} = (1 - f - 1/K_r)/f$. Consequently, the parameter K_r can be found as

$$K_r = \frac{1}{1 - fy_{0,2} - f} \qquad (11)$$

The main useful feature of the $y(x)$ dependence is its nonlinearity within the whole range of x. As shown in the inset of Figure 1, the slope of the curve increases with increasing x and levels off at large x (when $x \gg N/f$, see below). Equations 9 and 11 permit the determination of the fraction of protein-accessible lipids, f, and the relative affinity of the labeled versus unlabeled lipids for the protein, K_r, using y intercepts $y_{0,1}$ and $y_{0,2}$ of the tangents to this curve at $x \rightarrow 0$ and $x \gg N/f$. The affinity constant of the protein to the membrane (K) and the lipid-to-protein stoichiometry (N) can be determined using the slopes of these two tangents, which can be found by differentiation of eq 8 with respect to x:

$$\frac{dy}{dx} = \frac{1}{2fNK_r}\left(b + \frac{ab - 2fN}{\sqrt{a^2 - 4fNx}}\right) \qquad (12)$$

where $b \equiv f + N/KL_t$.

The limits of dy/dx at $x \rightarrow 0$ and $x \rightarrow \infty$ can be found from eq 12 as

$$\lim_{x \rightarrow 0} \frac{dy}{dx} = \frac{1}{fK_rKL_t} \qquad (13)$$

$$\lim_{x \rightarrow \infty} \frac{dy}{dx} = \frac{1}{fK_rKL_t} + \frac{1}{K_rN} \qquad (14)$$

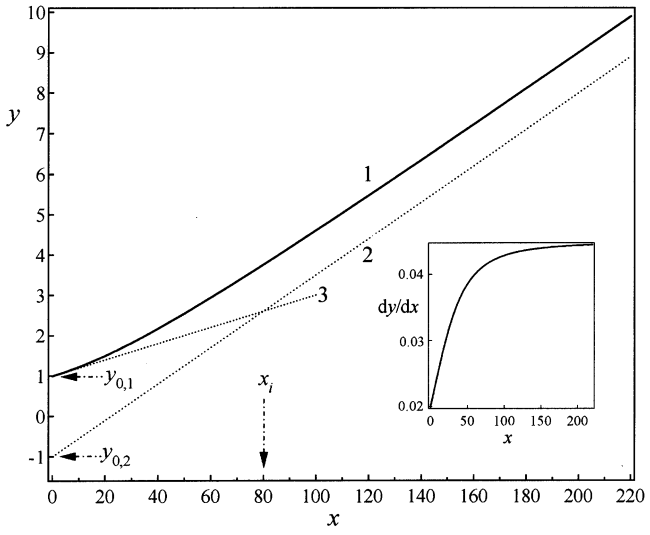

Figure 1. Dependence of the mole ratio of free to protein-bound lipids (y) on the overall lipid-to-protein ratio (x) simulated through eq 8 using the parameters $f = 0.5$, $K_r = 1$, $N = 40$, $K = 10^5$ M^{-1}, and $L_t = 10^{-3}$ M (line 1). Lines 2 and 3 are the tangents to curve 1 at very large x and at $x \rightarrow 0$, respectively (lines 1 and 2 merge at $x > 2000$). The meanings of the intercepts $y_{0,1}$ and $y_{0,2}$ are explained in the text, and x_i is the lipid-to-protein molar ratio corresponding to the intersection of tangents 2 and 3. The inset demonstrates the dependence of the slope of curve 1 on x.

The combination of eqs 13 and 14 with eqs 9 and 11 provides the following equations for the two tangents to the $y(x)$ dependence. At $x \rightarrow 0$,

$$y = \frac{x}{fK_rKL_t} + \frac{1}{f} - 1 \qquad (15)$$

and at $x \rightarrow \infty$,

$$y = \left(\frac{1}{fK_rKL_t} + \frac{1}{K_rN}\right)x + \frac{1}{f} - \frac{1}{fK_r} - 1 \qquad (16)$$

From eqs 15 and 16, we find that the two tangents intersect at

$$x_i = \frac{N}{f} \qquad (17)$$

Thus, for determination of the parameters f, K_r, K, and N, the tangents to the $y(x)$ dependence should be constructed at large and small x (as follows from eq 17, the criteria for "large" and "small" x are respectively $x \gg N/f$ and $x \ll N/f$). The intersections of these lines with the y axis are used in finding f and K_r by eqs 9 and 11, and their slopes are used in finding K and N by eqs 13 and 14. The values of these parameters may be verified using additional relationships that are obtained by an analysis of the dependence of the fraction of protein-bound lipids [$r_b = 1/(1 + y)$] on the lipid-to-protein ratio (x). It follows from eq 8 that at high protein concentrations ($x \rightarrow 0$), $y_{x \rightarrow 0} = 1/f - 1$. Consequently, $r_{b,x \rightarrow 0} = 1/(1 + y_{x \rightarrow 0}) = f$. Thus, as shown in Figure 2, the fraction of protein-accessible lipids (f) can be found directly by extrapolating the $r_b(x)$ dependence to the r_b axis:

$$f = r_{b,x \rightarrow 0} \qquad (18)$$

Furthermore, taking into account that $dr_b/dx = -(1 + y)^{-2}\, dy/dx$, that the limit of y at $x \rightarrow 0$ is $1/f - 1$ (see eq 8), and that the limit of dy/dx at $x \rightarrow 0$ is $1/fK_rKL_t$ (see eq 13), we obtain

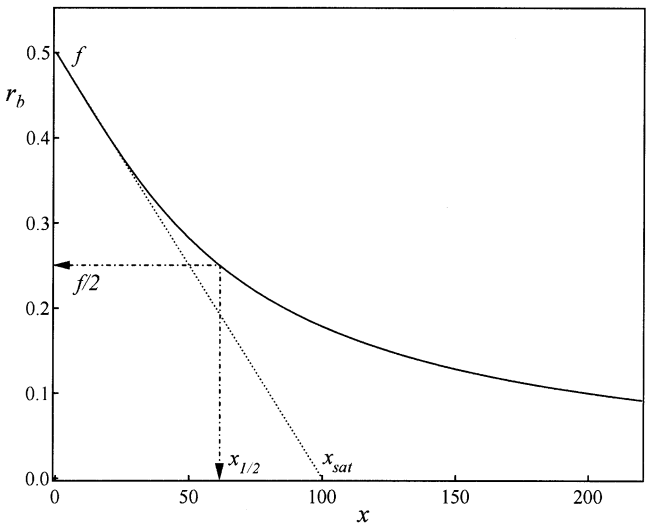

Figure 2. Dependence of the fraction of immobilized lipid (r_b) on the overall lipid-to-protein ratio (x) (—) simulated through eq 8 [$r_b = 1/(1 + y)$] using the parameters specified in Figure 1. $x_{1/2}$ is the lipid-to-protein ratio corresponding to half-saturation of protein binding, and x_{sat} is the x intercept of the tangent to the $r_b(x)$ curve at low x.

$$\lim_{x\to 0}\frac{dr_b}{dx} = -\frac{f}{K_r K L_t} \tag{19}$$

Equations 18 and 19 indicate that the equation for the tangent to the $r_b(x)$ curve at $x \to 0$ is

$$r_b = -\frac{f}{K_r K L_t}x + f \tag{20}$$

The coordinate of the intersection of this line with the x axis is

$$x_{sat} = K_r K L_t \tag{21}$$

Thus, the intersections of the tangent to the $r_b(x)$ curve at $x \to 0$ with the r_b and x axes permit the determination of the parameter f and the product $K_r K$ using eqs 18 and 21, respectively.

At half-saturation of protein binding (i.e., at $r_b = f/2$), $y = 2/f - 1$. Inserting this into eq 4, we get

$$n_b = N(1 + K_r) \tag{22}$$

Combination of eqs 5 and 22 yields

$$1 + K_r = \frac{1 + KP_{f,1/2}}{KP_{f,1/2}} \tag{23}$$

After making the following substitutions—$P_{f,1/2} = P_{t,1/2} - P_{b,1/2}$, $P_{t,1/2} = L_t/x_{1/2}$, and $P_{b,1/2} = fL_t/N(1 + K_r)$—where the subscript 1/2 indicates half-saturation of the protein binding, we obtain

$$N(1 + K_r) = \frac{fK_r K L_t x_{1/2}}{K_r K L_t - x_{1/2}} \tag{24}$$

Equations 21 and 24 yield

$$N(1 + K_r) = \frac{fx_{1/2}x_{sat}}{x_{sat} - x_{1/2}} \tag{25}$$

Equations 18, 21, and 25 can be used to refine the values of the parameters f, K_r, K, and N on the basis of $r_{b,x\to 0}$, $x_{1/2}$, and x_{sat}, as illustrated in Figure 2.

Next, we determine the fraction of the labeled lipids with respect to the total number of lipid molecules associated with a membrane-bound protein (n_r) and the microscopic Gibbs free energies of protein binding of labeled (ΔG_{lab}) and unlabeled lipids (ΔG_{unlab}). The labeled and unlabeled lipids are competing for binding to the protein, which can be described as follows:[19]

$$L_b = \frac{NkL_f}{1 + kL_f + k^*L_f^*} \tag{26}$$

$$L_b^* = \frac{Nk^*L_f^*}{1 + kL_f + k^*L_f^*} \tag{27}$$

where k and k^* are the microscopic binding constants of the unlabeled and labeled lipids for the protein, respectively. It follows from eqs 26 and 27 that the ratio of the binding constants of the labeled and unlabeled lipids for the protein is

$$\frac{k^*}{k} = \frac{L_b^* L_f}{L_f^* L_b} = K_r \tag{28}$$

From eqs 26−28, we have $L_b^*/(N - L_b^*) = K_r L_f^*/L_f$, or using the approximation $L_f^*/L_f = \theta/(1 - \theta)$, where θ is the overall fraction of the labeled lipids in the membrane with respect to the total lipids, we obtain

$$n_r \equiv \frac{L_b^*}{N} = \frac{K_r\dfrac{\theta}{1-\theta}}{1 + K_r\dfrac{\theta}{1-\theta}} \tag{29}$$

The protein-binding energies of the labeled and unlabeled lipids are found as follows. The protein-to-membrane binding constant can be presented as

$$K = \frac{1}{55.5}\exp(-\Delta G_t/RT) \tag{30}$$

where R is the universal gas constant, T is the absolute temperature, ΔG_t is the total energy of the protein binding to the membrane, and 55.5 is the total molar concentration of all components, including water, which appears when mole fractions are converted to molar concentrations. Obviously, ΔG_t is the sum of the energies of the interactions of all lipids with the protein, which, together with eq 30, yields

$$-RT \ln 55.5K = L_b^*\Delta G_{lab} + (N - L_b^*)\Delta G_{unlab} \tag{31}$$

Taking into account eqs 28 and 30, we have

$$K_r = \exp[(\Delta G_{unlab} - \Delta G_{lab})/RT] \tag{32}$$

After extracting ΔG_{unlab} from eq 32 and inserting it into eq 31, we get

$$\Delta G_{lab} = -RT\left[\frac{\ln 55.5K}{N} + (1 - n_r)\ln K_r\right] \tag{33}$$

Having determined ΔG_{lab}, we find ΔG_{unlab} from eq 32.

Materials and Methods

Materials. PLA_2 was purified from the venom of the snake *Agkistrodon piscivorus piscivorus* (Sigma, St. Louis, MO), as previously described.[20,21] Briefly, the crude protein was dis-

solved in an aqueous buffer (0.1 M NaCl, 10 mM Tris/HCl, pH 7.4) and, after removal of water-insoluble precipitates by centrifugation, was eluted from a Sephadex G-50 column using the same buffer. The protein peak corresponding to 14 kDa was pooled, lyophilized, dissolved in 0.1 M NaCl, 5 mM sodium phosphate (pH 6.8), loaded onto a SP-Sephadex C-50 column, and eluted using a 0.1 to 0.5 M linear NaCl concentration gradient. This yielded two protein peaks corresponding to the active AppD49 and inactive AppK49 PLA_2 isoforms, which were distinguished by activity assay. The AppD49 isoform was used in all experiments. Covalent inhibition of PLA_2 by *p*-bromophenacyl bromide (pBPB) was performed as described earlier.[22,23] The lipids were purchased from Avanti Polar Lipids (Alabaster, AL), and the other chemicals were obtained from Sigma (St. Louis, MO).

PLA_2 Concentration and Activity Measurements. Protein concentration was measured by Bradford assay.[24] PLA_2 activity against 1,2-diheptanoylthio-*sn*-glycero-3-phosphocholine (DHTPC) was measured spectrophotometrically using the $sPLA_2$ activity kit from Cayman Chemical (Ann Arbor, MI). As originally described by Reynolds et al.,[25] hydrolysis of the *sn*-2 thioester bond of DHTPC by PLA_2 is followed by the exposure of free thiols and conversion of 5,5′-dithio-bis-(2-nitrobenzoic acid) to 5-thio-nitrobenzoic acid, which is detected by absorbance at 412 nm.

EPR Experiments. Stock lipid suspensions with a total lipid concentration of 10 mM were prepared by extrusion through a 100-nm pore size polycarbonate membrane, as described,[18] using 97.5 mol % 1-palmitoyl-2-oleoyl-*sn*-glycero-3-phosphocholine (POPC) and 2.5 mol % 1-palmitoyl-2-oleoyl-*sn*-glycero-3-phospho-TEMPO-choline (POPTC) in 10 mM Hepes (pH 8.0) + 100 mM NaCl + 15 mM KCl buffers containing either 2 mM $CaCl_2$ or 0.5 mM EGTA without added $CaCl_2$. Certain volumes of the extruded vesicles were then mixed with appropriate amounts of the buffer and with 0.6 mM PLA_2 solutions in the same buffer to yield a constant lipid concentration of 1.4 mM and desired lipid-to-protein molar ratios. This corresponds to a 35 μM spin-labeled lipid concentration; considerably lower concentrations (e.g., <10 μM) of the spin-labeled lipid yielded unacceptably noisy spectra. Samples for EPR experiments were contained in sealed quartz capillaries (0.6-mm inner diameter) purchased from VitroCom (Mountain Lakes, NJ). Spin-label EPR experiments were performed at 22 °C using a Bruker EMX X-band EPR spectrometer at 2-mW microwave power. Spectra were acquired using 100-kHz field modulation with a peak-to-peak modulation amplitude of 1 G.

EPR Data Analysis. The fraction of the lipid in vesicles that was motionally restricted upon interaction with PLA_2 was determined as follows. The spectrum of the fluid POPC/POPTC membranes in the absence of PLA_2 was measured and considered to be a spectrum of the "free" lipid (see Figure 3). Increasing concentrations of PLA_2 resulted in two-component spectra. All first derivative spectra were integrated and curve-fitted using LabCalc software. Curve-fitting of the integrated spectrum of the free lipid revealed three major absorption peaks corresponding to the hyperfine interaction of the unpaired electron spin ($s = 1/2$) with the ^{14}N nuclear spin ($m_I = +1, 0, -1$) of the nitroxide group of POPTC. The low-field and central extrema were 75−92% Lorentzian and had full widths at half-height of 6.1−6.4 G, whereas the high-field peak was broader by ~5.5 G and incorporated an increased fraction of Gaussian components. With increasing PLA_2 concentration under non-catalytic conditions (0.5 mM EGTA), the intensities of the initially observed components were decreased, and new spectral components were detected with increasing intensities. The first derivative spectrum of the sum of the new components, produced by PLA_2, revealed decreased time averaging of the anisotropy (i.e., broadening of the external wings of the spectrum) and therefore was ascribed to motionally restricted, "bound" lipid (Figure 3). The integrated spectra corresponding to both free and bound lipids were normalized to yield similar areas and were differentiated. Fractions of these first derivative spectra were then used to fit the experimental spectra, which permitted the determination of the fraction of immobilized lipids at each PLA_2 concentration.

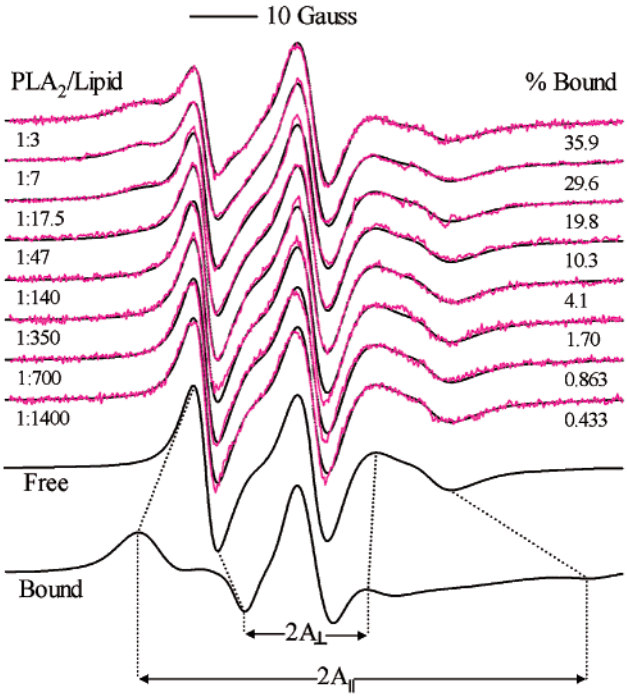

Figure 3. Experimental (magenta) and simulated (black) EPR spectra of vesicles composed of 97.5 mol % POPC and 2.5 mol % POPTC in the absence and presence of increasing concentrations of PLA_2 in a buffer containing 100 mM NaCl, 15 mM KCl, 0.5 mM EGTA, and 10 mM Hepes (pH 8.0). The spectra labeled "Free" and "Bound" are simulated as described in the text and correspond to membrane lipid components free of PLA_2 and bound to PLA_2, respectively. PLA_2/lipid molar ratios are shown on the left-hand side, and the fractions of the spectrum corresponding to the bound lipid that were added to the spectrum of the free lipid to obtain a best fit with the experiment are shown on the right-hand side.

The order parameters of free and bound lipids were determined as follows. Assuming that the *x* and *y* components of the hyperfine tensor are similar ($A_{xx} = A_{yy}$), which is well justified for nitroxide spin-labeled lipids,[26−29] the parallel and perpendicular components of the hyperfine tensor can be presented as

$$A_{||} = a_0 + \frac{2}{3}(A_{zz} - A_{yy})S_{zz} \tag{34}$$

$$A_{\perp} = a_0 - \frac{1}{3}(A_{zz} - A_{yy})S_{zz}, \tag{35}$$

where

$$S_{zz} = \frac{1}{2}\langle 3\cos^2\gamma - 1\rangle \tag{36}$$

$$a_0 = \frac{1}{3}(A_{zz} + 2A_{yy}) \tag{37}$$

A_{xx}, A_{yy}, and A_{zz} are the hyperfine tensor elements for isotropic motion. S_{zz} is the order parameter that characterizes "wobbling in a cone" of the lipid molecule with a half-amplitude of γ.[26,30] Equations 34 and 35 yield

$$S_{zz} = \frac{A_{||} - A_{\perp}}{A_{zz} - A_{yy}} \tag{38}$$

For TEMPO in water at 22 °C, the parameters a_0 and A_{zz} have been determined to be 17.32 and 38.0 G, respectively.[31] After inserting these values into eq 37, we obtain $A_{zz} - A_{yy} = 31.02$ G, which, along with experimentally determined hyperfine tensor components $A_{||}$ and $A_{\perp}$ (see Figure 3), permit the determination of S_{zz} by eq 38.

Results

Binding of PLA_2 to Membranes under Noncatalytic Conditions. EPR spectra of POPC vesicles containing 2.5 mol % POPTC were measured at a constant lipid concentration (1.4 mM) in the absence and in the presence of increasing concentrations of PLA_2. Under noncatalytic conditions (0.5 mM EGTA), two-component spectra have been obtained. A decrease in intensity of the outer lines and the appearance of new spectral components at both lower- and higher-field wings of the spectra indicate that the second component has an increased outer hyperfine splitting and likely results from partial immobilization of the lipid upon interaction with PLA_2 (Figure 3). Comparison of the spectra of the free and immobilized (bound) lipids, which were identified as described in the preceding section, indicates an increase in $A_{||}$ from 19.4 to 33.9 G and a decrease in $A_{\perp}$ from 12.0 to 9.1 G upon immobilization. This allows the determination of the order parameters of the free and immobilized lipids through eq 38 as $S_{zz,free} = 0.24$ and $S_{zz,bound} = 0.80$, respectively.

The experimental spectra were fitted by a combination of spectra of the free and bound lipids, which yielded the fractions of the bound lipid (r_b) at each PLA_2 concentration, as shown on the right-hand side of Figure 3. The parameters f, K_r, K, and N characterizing PLA_2 binding to membranes have been evaluated using the dependence of y [$= (1 - r_b)/r_b$] on the overall lipid-to-protein molar ratio, x (Figure 4). As shown in the inset 1 of Figure 4, the $y(x)$ plot crosses the y axes at $y_{0,1} \approx 1.3$. Insertion of this value into eq 9 yields $f \approx 0.43$. The value of f has also been determined using the dependence of r_b on x, as described above (eq 18), and yielded a similar result (not shown). Evaluation of K_r requires $y_{0,2}$ (i.e., the y intercept of the extrapolation of the linear part of the $y(x)$ dependence) corresponding to large x. Inset 2 of Figure 4 shows that at $x \geq 100$ the slope of the $y(x)$ dependence approaches a limiting level. Therefore, the data points corresponding to $x = 350$, 700, and 1400 can be used to extrapolate the plot to the y axis and find $y_{0,2}$. The values of y corresponding to these values of x are 57.80, 114.87, and 229.95, respectively, implying that $y_{0,2} \approx 0$. Using $y_{0,2} = 0$ and $f = 0.43$ in eq 11, we obtain $K_r \approx 1.75$.

For the evaluation of K and N, we need the slopes of the $y(x)$ dependence at small and large x. (As specified above, small and large x means $x \ll N/f$ and $x \gg N/f$, respectively). The values of y at $x = 3$ and 7 are respectively 1.785 and 2.378, implying that dy/dx at small x is 0.148 (see also inset 2 of Figure 4). Inserting this value of dy/dx into eq 13, in conjunction with the values of f and K_r determined above and $L_t = 1.4$ mM, we find that $K \approx 6.41$ mM^{-1}. The values of y at $x = 350$, 700, and 1400 (see above) indicate that dy/dx at large x is 0.1637, which allows us to determine that the lipid-to-protein stoichiometry from eq 14 is $N = 36.4$.

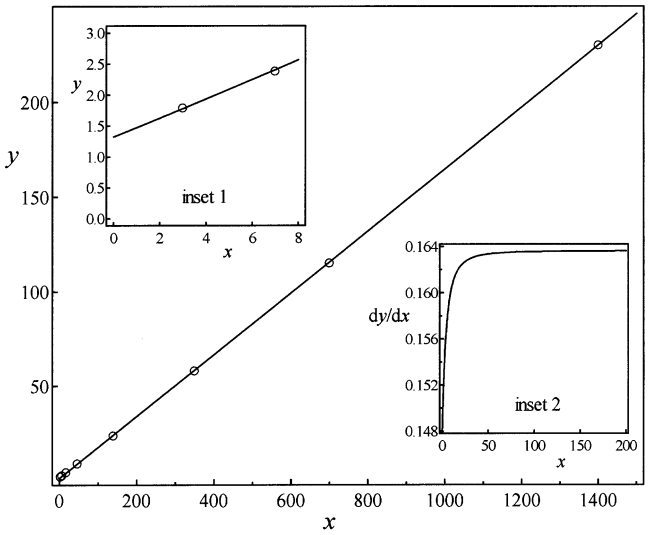

Figure 4. Experimental and simulated dependence of the mole ratio of free to protein-bound lipids (y) on the overall lipid-to-protein ratio (x). The data points are deduced from the results of Figure 3. The solid line is simulated through eq 8 using the parameters $f = 0.43$, $K_r = 1.75$, $N = 36.4$, $K = 6.41 \times 10^3$ M^{-1}, and $L_t = 1.4$ mM, which yield the best fit with the experimental data (○). Inset 1 is a magnification of the data in the low x region to show the y intercept of the $y(x)$ dependence, which was used to evaluate f through eq 9. Inset 2 demonstrates the change of the slope of the $y(x)$ dependence in the region $0 \leq x \leq 200$.

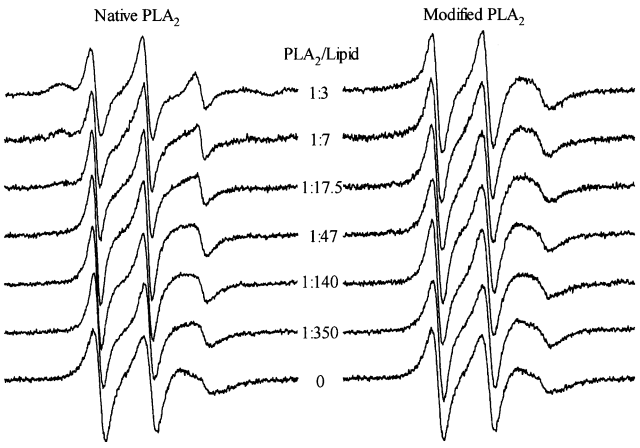

Figure 5. EPR spectra of vesicles composed of 97.5 mol % POPC and 2.5 mol % POPTC in the absence and presence of native (left) and pBPB-modified PLA_2 (right) at PLA_2-to-lipid molar ratios shown in the center. The buffer contained 100 mM NaCl, 15 mM KCl, 2 mM $CaCl_2$, and 10 mM Hepes (pH 8.0).

Using $N = 36.4$, $K_r = 1.75$, and $\theta = 0.025$ in eq 29, we find that the number of labeled lipids bound to PLA_2 is $L_b^* = 1.56$, implying that, on average, every 2 membrane-bound PLA_2 molecules interact with 3 labeled lipids and 70 unlabeled lipids. Furthermore, using $n_r \approx 0.0429$ (see eq 29), we obtain through eqs 33 and 32 $\Delta G_{lab} \approx -0.887RT \approx -516$ cal/mol and $\Delta G_{unlab} \approx -0.327RT \approx -190$ cal/mol.

Having determined N and ΔG_{unlab}, the binding constant of PLA_2 for pure POPC membranes (K_{POPC}) can be evaluated by using $\Delta G_t = N\Delta G_{unlab}$ in eq 30. This yields $K_{POPC} = 2661$ M^{-1}.

Interaction of PLA_2 with Membranes under Catalytic Conditions. POPC/POPTC membranes in the presence of PLA_2 under catalytic conditions (i.e., in the presence of 2 mM $CaCl_2$) generated complex EPR spectra. At high PLA_2/lipid ratios, at

TABLE 1: Parameters Characterizing PLA_2−Membrane Interactions

$S_{zz,free}$ (order parameter of membrane lipids free of PLA_2)	0.24
$S_{zz,bound}$ (order parameter of membrane lipids bound to PLA_2)	0.80
f (fraction of protein-accessible lipids)	0.43
K (binding constant of PLA_2 for POPC/POPTC membranes)	6410 M^{-1}
K_{POPC} (binding constant of PLA_2 for pure POPC membranes)	2661 M^{-1}
K_r (relative binding constant of the labeled vs unlabeled lipid for PLA_2)	1.75
N (total number of lipid molecules interacting with a PLA_2 molecule)	36.4
n_r (fraction of labeled lipids interacting with a PLA_2 molecule)	0.0429
ΔG_{unlab} (Gibbs free energy of interaction of an unlabeled lipid with PLA_2)	−190 cal/mol
ΔG_{lab} (Gibbs free energy of interaction of a labeled lipid with PLA_2)	−516 cal/mol

least three motionally distinct lipid components are evident. In addition to an immobilized lipid component, described above, increasing PLA_2 concentrations substantially affect the shape of the high-field resonance line (Figure 5, left). The peak of this component becomes progressively sharper and moves farther from the central line, corresponding to an increase in $A_\perp$ and, consequently, a lower-order parameter S_{zz} (see eq 38). Thus, binding of PLA_2 to the membranes under conditions allowing lipid hydrolysis induces lipid components with both restrained and increased motional freedom. The immobilized lipid component evidently results from the binding of PLA_2 to the membrane surface by the same mechanisms that operate under noncatalytic conditions (see preceding section). Because the mobile lipid component arises only under catalytic conditions, it probably reflects the hydrolytic activity of PLA_2. To verify this, similar experiment were carried out using PLA_2, which was covalently modified by pBPB and has been shown to be completely inactive.[32] The presence of this inhibited PLA_2 had only a minor effect on the high-field resonance line (Figure 5, right). These results suggest that the lipid component with increased mobility that results from the action of native PLA_2 under catalytic conditions likely reflects lipid hydrolysis and membrane destabilization. It should be noted, however, that the lipid immobilizing effect of the inhibited PLA_2 is much weaker than that of the native PLA_2, which strongly suggests that the covalently modified PLA_2 does not bind to the membranes as strongly as the native PLA_2 binds.

Discussion

Thus far, the protein−lipid interactions have been characterized by spin-label EPR spectroscopy using a formalism for integral proteins, which permitted the determination of the parameters K_r and N (i.e., the relative affinity of the labeled versus unlabeled lipid for the protein and the lipid-to-protein binding stoichiometry, respectively). The present study offers experimental and theoretical approaches that allow a comprehensive analysis of membrane binding of peripheral proteins. Application of the theory to EPR experiments on the binding of a secretory PLA_2 to membranes containing a spin-labeled lipid yields all key parameters that determine the membrane binding of PLA_2 (see Table 1). The discussion provided below shows that the values of these parameters make good physical sense, which confirms the validity of the new theory.

It is important to estimate the limits of deviations of binding parameters K, N, f, and K_r from their best-fit values, which still allow reasonable fitting with the experiment. The binding constant K is determined from the slope of the $y(x)$ dependence at high protein concentration (see eq 13), when the effect of lipid immobilization is strong and can be measured reliably. Analysis showed that the variation of K within limits of no more than ±10% still yields a reasonably good fit (i.e., $K = 6410 \pm 600$ M^{-1}). The theoretical $y(x)$ dependence is also very sensitive to f and K_r; these parameters can diverge from the mean values only by approximately 5−8%. However, alterations of N within limits of up to ±30% are permissible in terms of fitting the experimental data (i.e., $N \approx 36 \pm 10$). Although the situation is not as satisfying with N as with the other parameters, the overall usefulness of the method for the determination of binding parameters is remarkable, especially considering the power of the method in terms of the number of evaluated parameters.

Taking into account the dimensions of extruded unilamellar vesicles (∼100 nm in diameter) and the membrane thickness, (∼4 nm), the fraction of the lipid in the outer leaflets of membranes, which is accessible to externally added PLA_2, is $(R^2/r^2)/(1 + R^2/r^2) \approx 0.54$, where $R = 50$ nm and $r = 46$ nm are the external and internal radii of the vesicles, respectively. However, because of the irregular shape of the protein, even at the saturation of protein binding there is an excluded area that is not accessible to the protein. For example, if the membrane-binding surface of PLA_2 is modeled with an ellipse of arbitrary semiaxes, then the fraction of the excluded area per PLA_2 is $1 - \pi/4$ (i.e., the fraction of the protein-accessible area is $\pi/4 \approx 0.785$). This implies that the overall PLA_2-accessible area would be $\sim 0.54 \times 0.785 \approx 0.42$, which is consistent with the value of $f = 0.43$ that was evaluated above for the fraction of protein-accessible lipids.

The number of phospholipid molecules interacting with a membrane-bound PLA_2 (N) has been determined for various isoforms of group I/II PLA_2s and varied within the limits of 25 to 50.[5,33−38] The value of $N \approx 36 \pm 10$ obtained in this work is in good agreement with these results. The present data suggest that, on average, ∼4.3% of these molecules are labeled lipids and the rest are unlabeled lipids.

The binding constant of AppD49 for polymerized 1,2-bis-[12-(lipoyloxy)dodecanoyl]-*sn*-glycero-3-hosphocholine vesicles was measured previously by fluorescence spectroscopy to be $<10^3$ M^{-1}.[39] A similar method was used to determine $K = 360$ M^{-1} and 7700 M^{-1} for the binding of AppD49 to the outer surfaces of large (100−120 nm) and small (25−30 nm) unilamellar vesicles of 1,2-dipalmitoyl-*sn*-glycero-3-phosphocholine (DPPC) in the solid phase.[38] The binding constant of PLA_2 for fluid POPC membranes determined here ($K_{POPC} = 2661$ M^{-1}) is closer to the binding constant obtained for small DPPC vesicles. This may be accounted for by the fact that higher curvature is equivalent to a decreased packing density of lipid molecules in the outer leaflets of membranes, which mimics the fluid phase.

The present data indicate an increased affinity of the spin-labeled POPTC lipid for PLA_2 compared to that of POPC ($K_r = k^*/k = 1.75$). This probably results from hydrophobic interactions between the tetramethyl group of TEMPO and the protein and is consistent with earlier findings that hydrophobic interactions significantly contribute to PLA_2−membrane interactions.[35,37,40]

Comparison of data under noncatalytic (Figure 3) and catalytic conditions (Figure 5, left) at high PLA_2 concentrations

shows that in both cases two motionally distinct populations are clearly resolved. However, the low-field lines, which are most sensitive to the exchange kinetics between the bound- and free-lipid populations,[41] are broader under noncatalytic conditions. This implies that although in both cases the system is in the slow-exchange regime ($\sim 5 \times 10^{-8}$ s) the exchange rate is moderately increased under noncatalytic conditions. This may result from tighter binding of the lipid to PLA_2 under catalytic conditions, which is consistent with the notion that Ca^{2+} increases the affinity of phospholipids for PLA_2.[42,43] The presence of the sharp high-field line under catalytic conditions at high PLA_2 concentrations, however, cannot be attributed to a decreased exchange rate between the bound- and free-lipid populations because (i) the high-field line is less sensitive to exchange than the low-field line and (ii) this line is distinctly different (sharper) from that in the spectrum of pure lipid (i.e., in the absence of exchange). The sharp high-field line can be interpreted only in terms of the appearance of a new lipid population with increased mobility. Lipid hydrolysis by PLA_2 is likely to produce distinct populations of spin-labeled lysophospholipid (a) in the membrane not interacting with PLA_2, (b) in the membrane interacting with PLA_2, (c) dissociated from the membrane in a monodisperse form, and (d) dissociated from the membrane in micellar form. A fraction of the lysolipid may also be bound to the catalytic site of PLA_2 both at the membrane surface and in the solution. Although this creates enormous complexity, which prohibits quantitative analysis of the spectra under catalytic conditions, the present data clearly demonstrate that PLA_2 activity can be detected by spin-label EPR.

In conclusion, we demonstrate in this work that the interactions of peripheral proteins with membranes can be characterized in detail on the basis of the influence of the protein on the line shape of EPR spectra. POPTC turned out to be an excellent choice for spin-labeled lipids; lipids with spin-labeled hydrocarbon chains are not sufficiently sensitive to protein binding at the membrane surface.[44,45] Moreover, the present results demonstrate how the activity of lipolytic enzymes can be monitored by EPR. These results provide new prospects in the characterization of protein−membrane interactions by biophysical methods.

Acknowledgment. This work was supported by NIH grant HL65524.

References and Notes

(1) Exton, J. H. *Biochim. Biophys. Acta* **1998**, *1436*, 105−115.
(2) Lennartz, M. R. *Int. J. Biochem. Cell Biol.* **1999**, *31*, 415−430.
(3) Griffith. O. H.; Ryan, M. *Biochim. Biophys. Acta* **1999**, *1441*, 237−254.
(4) Huijbregts, R. P.; Topalof, L.; Bankaitis, V. A. *Traffic* **2000**, *1*, 195−202.
(5) Berg, O. G.; Gelb, M. H.; Tsai, M.-D.; Jain, M. K. *Chem. Rev.* **2001**, *101*, 2613−2653.
(6) Newton, A. C. *Methods Enzymol.* **2002**, *345*, 499−506.
(7) Brophy, P. J.; Horváth, L. I.; Marsh, D. *Biochemistry* **1984**, *23*, 860−865.
(8) Knowles, P. F.; Watts, A.; Marsh, D. *Biochemistry* **1979**, *18*, 4480−4487.
(9) Ellena, J. F.; Blazing, M. A.; McNamee, M. G. *Biochemistry* **1983**, *22*, 5523−5535.
(10) Horváth, L. I.; Brophy, P. J.; Marsh, D. *Biochemistry* **1988**, *27*, 46−52.
(11) Kleinschmidt, J. H.; Powell, G. L.; Marsh, D. *Biochemistry* **1998**, *37*, 11579−11585.
(12) Rietveld, A.; Berkhout, T. A.; Roenhorst, A.; Marsh, D.; de Kruijff, B. *Biochim. Biophys. Acta* **1986**, *858*, 38−46.
(13) Sankaram, M. B.; Brophy, P. J.; Jordi, W.; Marsh, D. *Biochim. Biophys. Acta* **1990**, *1021*, 63−69.
(14) Kleinschmidt, J. H.; Marsh, D. *Biophys. J.* **1997**, *73*, 2546−2555.
(15) Kleinschmidt, J. H.; Mahaney, J. E.; Thomas, D. D.; Marsh, D. *Biophys. J.* **1997**, *72*, 767−778.
(16) Victor, K. G.; Cafiso, D. S. *Biophys. J.* **2001**, *81*, 2241−2250.
(17) Brotherus, J. R.; Griffith, O. H.; Brotherus, M. O.; Jost, P. C.; Silvius, J. R.; Lowell, E. H. *Biochemistry* **1981**, *20*, 5261−5267.
(18) Tatulian, S. A. *Biophys. J.* **2001**, *80*, 789−800.
(19) Tatulian, S. A. In *Surface Chemistry and Electrochemistry of Membranes*; Sørensen, T. S., Ed.; Marcel Dekker: New York, 1999; pp 871−922.
(20) Maraganore, J. M.; Merutka, G.; Cho, W.; Welches, W.; Kézdy, F. J.; Heinrikson, R. L. *J. Biol. Chem.* **1984**, *259*, 13839−13843.
(21) Cho, W.; Shen, Z. In *Lipase and Phospholipase Protocols*; Doolittle, M., Reue, K., Eds.; Humana Press: Totowa, NJ, 1999; pp 303−307.
(22) Halpert, J.; Eaker. D.; Karlsson, E. *FEBS Lett.* **1976**, *61*, 72−76.
(23) Yang, C. C.; King, K. *Biochim. Biophys. Acta* **1980**, *614*, 373−388.
(24) Bradford, M. M. *Anal. Biochem.* **1976**, *72*, 248−254.
(25) Reynolds, L. J.; Hughes, L. L.; Dennis, E. A. *Anal. Biochem.* **1992**, *204*, 190−197.
(26) Hubbell, W. L.; McConnell, H. M. *J. Am. Chem. Soc.* **1971**, *93*, 314−326.
(27) Freed, J. H. In *Spin Labeling: Theory and Applications*; Berliner, L. J., Ed.; Academic Press: New York, 1976; pp 53−132.
(28) Gaffney, B. J. *Methods Enzymol.* **1974**, *32*, 161−198.
(29) Marsh, D. In *Spectroscopy and the Dynamics of Molecular Biological Systems*; Bayley, P. M., Dale, R. E., Eds.; Academic Press: New York, 1985; pp 209−238.
(30) McConnell, H. M. In *Spin Labeling: Theory and Applications*; Berliner, L. J., Ed.; Academic Press: New York, 1976; pp 525−560.
(31) Windle, J. J. *J. Magn. Reson.* **1981**, *45*, 432−439.
(32) Tatulian, S. A.; Steczko, J.; Minor, W. *Biochemistry* **1998**, *37*, 15481−15490.
(33) Jain, M. K.; DeHaas, G. H.; Marecek, J. F.; Ramirez, F. *Biochim. Biophys. Acta* **1986**, *860*, 475−483.
(34) Dua, R.; Wu, S.-K.; Cho, W. *J. Biol. Chem.* **1995**, *270*, 263−268.
(35) Lee, B.-I.; Yoon, E. T.; Cho, W. *Biochemistry* **1996**, *35*, 4231−4240.
(36) Han, S. K.; Yoon, E. T.; Scott, D. L.; Sigler, P. B.; Cho, W. *J. Biol. Chem.* **1997**, *272*, 3573−3582.
(37) Sumandea, M.; Das, S.; Sumandea, C.; Cho, W. *Biochemistry* **1999**, *38*, 16290−16297.
(38) Gadd, M. E.; Biltonen, R. L. *Biochemistry* **2000**, *39*, 9623−9631.
(39) Shen, Z.; Wu, S.-K.; Cho, W. *Biochemistry* **1994**, *33*, 11598−11607.
(40) Stahelin, R. V.; Cho, W. *Biochemistry* **2001**, *40*, 4672−4678.
(41) Marsh, D.; Horváth, L. I. In *Advanced EPR: Applications in Biology and Biochemistry*; Hoff, A. J., Ed.; Elsevier: Amsterdam, 1989; pp 707−752.
(42) Scott, D. L.; Sigler, P. B. *Adv. Protein Chem.* **1994**, *45*, 53−88.
(43) Scott, D. L.; Sigler, P. B. *Adv. Inorg. Biochem.* **1994**, *10*, 139−155.
(44) Marsh, D. *FEBS Lett.* **1990**, *268*, 371−375.
(45) Marsh, D. *Biosci. Rep.* **1999**, *19*, 253−259.